Slow and stored light with atom-based squeezed light

Gleb Romanov, Travis Horrom, Eugeniy E. Mikhailov, and Irina Novikova

Department of Physics, College of William and Mary, Williamsburg,Virginia 23185, USA

ABSTRACT

In this manuscript we present calculations that consider the propagation of a squeezed vacuum signal field through a resonant atomic medium under electromagnetically induced transparency (EIT). We show that squeezing is degraded due to four-wave mixing processes at high optical depth of the atomic medium. We also present some preliminary results for degenerate Zeeman EIT resonances.

Keywords: electromagnetically induced transparency, quantum noise, four-wave mixing, squeezed vacuum

1. INTRODUCTION

In recent years, an increasing number of applications have improved their performance by harnessing the quantum mechanical properties of light. Quantum cryptography protocols rely on absolute security of data transmission encoded in quantum states of light.[1,2] Realization of long-distance quantum networks requires development of tools for manipulation and storage of quantum states.[3–7] Further, measurements with sensitivity beyond the standard quantum limit are possible[8–10] by replacing a standard laser probe with an optical field possessing modified quadrature noise, such as squeezed light.[8] Additionally, quantum sensors can be made that surpass their classical counterparts by using new measurement protocols based on quantum mechanical operators.[12] Many of the proposed and demonstrated realizations of these techniques rely on the ability to couple light to resonant systems, such as an ensemble of atoms (hot,[13–17] cold,[18–21] ultra-cold,[22,23] imbedded inside a solid state matrix[24–28]), quantum dots,[29,30] "atom-like" photonic structures[31–33] or plasmonic nanostructures.[33,34]

In the last decade, a lot of attention from both theorists and experimentalists has been focused on studies of interaction of light and atoms in a Λ-type configuration, in which two ground-state hyperfine levels are linked with a common excited state, as shown in Fig. 1. In this case, the control field $\Omega(t)$ strongly couples the propagation of the signal optical field $\mathcal{E}(z,t)$ with a collective long-lived ground-state atomic spin coherence (spin wave, defined below), resulting in electromagnetically induced transparency (EIT) and a reduced group velocity for signal pulses ("slow light").[35–37] Adiabatic turn-off of the control field maps the quantum state of the signal field onto the spin wave, which can be stored and later retrieved by restoring the control field intensity ("stored light"). Such an interaction scheme holds many promises for realizations of quantum memory, entanglement of distant atomic ensembles, few-photon level quantum gates, etc.

In the current manuscript we consider propagation of a quantum optical signal field under EIT conditions, taking into account the coherent four-wave mixing (FWM) due to off-resonant coupling of the control field.[38–41] Recent studies have demonstrated that this effect becomes important at high optical depth of an atomic ensemble, in which EIT offers maximum advantages.[43,44] Here we calculate the evolution of a quadrature squeezed signal field and demonstrate the deterioration of squeezing due to the four-wave mixing. We also investigate the quantum fluctuations of the generated Stokes field, and see that while it exhibits a phase-sensitive quantum noise, it does not become squeezed itself.

Send correspondence to: inovikova@physics.wm.edu

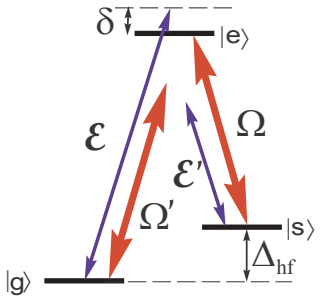

Figure 1. A typical double-Λ system used for modeling the EIT-FWM interaction.

2. PROPAGATION OF SIGNAL AND STOKES FIELDS UNDER EIT-FWM CONDITIONS

2.1 Classical fields

Several recent publications have shown that the simplified treatment of a single-Λ system is incomplete and, for example, fails to describe light storage at high optical depths.[38,41,43–45] In particular, it becomes important to take into account the off-resonant interaction of the strong classical control field, which resonantly drives the $|g\rangle - |e\rangle$ transition (see Fig. 1), but also acts on the $|s\rangle - |e\rangle$ transition with corresponding Rabi frequency Ω'. The atomic ground-state coherence enhances the spontaneous generation of a new Stokes optical field $\mathcal{E}'(z,t)$. If we assume that the hyperfine splitting between the two ground states $\Delta_h f$ is large compared to both the Rabi frequency and excited state linewidth γ, one can use a Floquet analysis[49] to adiabatically eliminate the off-resonant interaction. After a number of reasonable approximations (dipole approximation, rotating wave approximation under four-photon resonance conditions, the all atomic population in average is in $|g\rangle$),and to linear order in the weak light field amplitudes $\mathcal{E}$ and $\mathcal{E}'$, the atomic evolution and light propagation equations read:

$$(\partial_t + c\partial_z)\,\mathcal{E} = ig\sqrt{N}P, \tag{1}$$

$$(\partial_t + c\partial_z)\,\mathcal{E}'^{*} = -ig\sqrt{N}\frac{\Omega}{\Delta_{\rm hf}}S, \tag{2}$$

$$\partial_t S = -\Gamma_0 S + i\Omega P + i\frac{\Omega}{\Delta_{\rm hf}}g\sqrt{N}\mathcal{E}'^{*}, \tag{3}$$

$$\partial_t P = -\Gamma P + i\Omega S + ig\sqrt{N}\mathcal{E}. \tag{4}$$

Here we define the optical polarization $P(z,t) = \rho_{\rm eg}(z,t)\sqrt{N}$ and the spin coherence $S(z,t) = \rho_{\rm sg}(z,t)\sqrt{N}$, where $\rho_{ij}(z,t)$ is the appropriate slowly-varying position-dependent collective density matrix element, and N is the number of atoms in the interaction volume V. The coupling constant g, defined for a quantum field, can be connected to the classical optical depth $\alpha L = 3/(2\pi)\ \lambda^2(N/V)L$ of the atomic ensemble as $g\sqrt{N} = \sqrt{\gamma\alpha Lc/2}$. We also phenomenologically introduce $\Gamma = \gamma - i(\delta - 2|\Omega'|^2/\Delta_{\rm hf})$ and $\Gamma_0 = \gamma_0 - i(\delta - |\Omega'|^2/\Delta_{\rm hf})$ to be the decoherence rates of optical and spin polarizations correspondingly, where γ is the pressure-broadened optical transition linewidth, γ_0 is the ground state decoherence rate, and δ is a two-photon detuning between the signal and control fields. These expressions take into account small light shifts of the states $|e\rangle$ and $|g\rangle$ by $|\Omega'|^2/\Delta_{\rm hf}$ and $-|\Omega'|^2/\Delta_{\rm hf}$, respectively, due to the off-resonant coupling of the control field. Finally, for the relevant Clebsch-Gordon coefficients,[42] $\Omega' = -\sqrt{3}\Omega$.

These equations of motion reveal an interesting cause-and-effect relationship between the signal and Stokes optical fields and spin wave. Eq.(2) shows that the modifications in the Stokes field are determined by the spin wave. At the same time, some recent studies have shown[44] that under the broad range of reasonable experimental parameters, the collective ground-state spin coherence is determined predominantly by the signal optical field,

$$S(z,t) \approx -\frac{g\sqrt{N}}{\Omega}\mathcal{E}(z,t),. \tag{5}$$

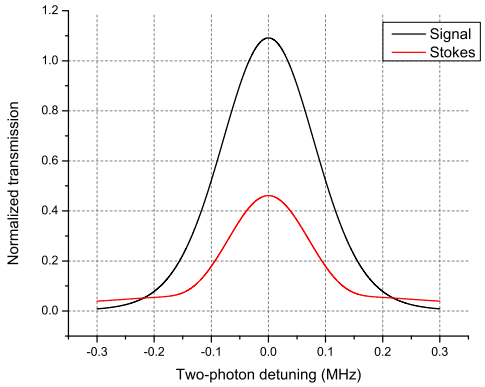

Figure 2. Calculated signal and Stokes fields after the interaction with atomic ensemble of optical depth $\alpha L = 40$ under EIT-FWM conditions as a function of two-photon detuning δ. We assumed a weak input signal field and no Stokes field. The shown transmission spectra are normalized to the input signal field amplitude. Used parameters: $\gamma = 2\pi$ 150 MHz, $\gamma_0 = 2\pi$ 270 Hz, $\Omega = 2\pi$ 9 MHz.

Eqs. (1-4) can then be solved analytically for both signal and Stokes optical fields, in the frequency domain:[38, 41, 43, 45]

$$\begin{pmatrix} \mathcal{E}(z,\omega) \\ \mathcal{E}'^{*}(z,\omega) \end{pmatrix} = e^{i\sigma z} \begin{pmatrix} \cosh(\xi z) + i\frac{\sigma}{\xi}\sinh(\xi z) & i\frac{2\Delta_{\rm R}}{\beta}\sinh(\xi z) \\ -i\frac{2\Delta_{\rm R}}{\beta}\sinh(\xi z) & \cosh(\xi z) - i\frac{\sigma}{\xi}\sinh(\xi z) \end{pmatrix} \begin{pmatrix} \mathcal{E}(0,\omega) \\ \mathcal{E}'^{*}(0,\omega) \end{pmatrix}, \tag{6}$$

where

$$\begin{aligned} \Delta_{\rm R} &= -\Omega^2/\Delta_{\rm hf},\ \beta = \sqrt{(\Gamma_0 - i\omega)^2 + 4\Delta_{\rm R}^2},\ \sigma = \frac{\alpha\gamma}{4F}(i\Gamma_0 + \omega),\ \xi = \frac{\alpha\gamma}{4F}\beta, \\ F &= \Omega^2 + (\Gamma - i\omega)(\Gamma_0 - i\omega). \end{aligned} \tag{7}$$

An example calculation of signal field transmission under the EIT-FWM conditions is presented in Fig. 2. Even though we assume no input Stokes amplitude (vacuum field), we observe significant growth in both Stokes and signal fields.

2.2 Quantum fields

The analysis of the effect of four-wave mixing on the propagation of the optical signal is not complete without evaluation of its quantum fluctuations. The propagation of quantized optical fields in a EIT-FWM medium can be described by equations similar to Eqs.(6), in which the mean values of the signal and Stokes optical field amplitudes $\mathcal{E}(z,t)$ and $\mathcal{E}'^{*}(z,t)$ are replaced with corresponding quantum operators $\hat{a}(z,t)$ and $\hat{b}(z,t)$:[46–48]

$$\begin{pmatrix} \hat{a}(z,\omega) \\ \hat{b}^{\dagger}(z,\omega) \end{pmatrix} = \begin{pmatrix} A(\omega) & B(\omega) \\ C(\omega) & D(\omega) \end{pmatrix} \left[\begin{pmatrix} \hat{a}(0,\omega) \\ \hat{b}^{\dagger}(0,\omega) \end{pmatrix} + \begin{pmatrix} \hat{F}_a(\omega) \\ \hat{F}_{b^{\dagger}}(\omega) \end{pmatrix} \right], \tag{8}$$

where A, B, C and D are the coefficients of the matrix given in Eq.(6), and $\hat{F}_a(\omega)$ and $\hat{F}_{b^{\dagger}}(\omega)$ are the Langevin force terms describing the effects of atomic dynamics on the signal and Stokes field propagation.[46] In the following treatment we neglect the contribution of the Langevin terms by restricting our analysis to the region of relatively small two-photon detunings δ, shown in Fig. 2. In this case, the absorption of the signal optical field is suppressed due to EIT conditions, and the Stokes optical field is far-detuned from any optical transition, and thus mostly insensitive to any resonant absorption, and the contribution of atomic noise is negligible.[47] However, the effect of atomic noise will be included in the future, more complete treatment.

We also need to introduce the quadrature operators $\delta\hat{x}$ and $\delta\hat{p}$ for both signal and Stokes optical fields, following the standard definitions. For the quantum signal field $\hat{a}$, the amplitude and phase quadratures are defined as:

$$\begin{aligned} \delta\hat{x}_a &= \hat{a}e^{-i\phi_a} + \hat{a}^\dagger e^{i\phi_a}, & (9)\\ \delta\hat{p}_a &= -i\left(\hat{a}e^{-i\phi_a} - \hat{a}^\dagger e^{i\phi_a},\right) & (10) \end{aligned}$$

and the analogous quadrature operators for the Stokes field are obtained by replacing $\hat{a}, \hat{a}^\dagger$ with $\hat{b}, \hat{b}^\dagger$. Here $\phi_{a,b}$ are quadrature phases; it is easy to see that $\delta\hat{x}_a(\phi_a = 0) = i\delta\hat{p}_a(\phi_a = \pi/2)$. The power spectra of these noise quadratures can then be measured experimentally using, for example, a homodyne detection,[11] described below in more detail. Theoretically, $S_{a,b}(\omega)$ is calculated as:

$$S_{a,out}(\omega)2\pi\delta(\omega-\omega') = \langle\delta\hat{x}_{a,out}(\omega)\delta\hat{x}^\dagger_{a,out}(\omega')\rangle \quad (11)$$

Using Eqs.(9,10) we can write $S_{a,out}(\omega)$ using expectation values for various combinations of $\hat{a}$ and $\hat{a}^\dagger$ operators:

$$\begin{aligned} S_{a,out}(\omega)2\pi\delta(\omega-\omega') &= \langle\delta\hat{a}_{out}(\omega)\delta\hat{a}^\dagger_{out}(-\omega')\rangle \\ &+ \langle\delta\hat{a}_{out}(\omega)\delta\hat{a}_{out}(-\omega')\rangle e^{-2i\phi_{a,out}} \\ &+ \langle\delta\hat{a}^\dagger_{out}(\omega)\delta\hat{a}^\dagger_{out}(-\omega')\rangle e^{2i\phi_{a,out}} \\ &+ \langle\delta\hat{a}^\dagger_{out}(\omega)\delta\hat{a}_{out}(-\omega')\rangle \quad (12) \end{aligned}$$

Then using Eq.(8) we can write the relationships between input and output quantum field operators:

$$\begin{aligned} \delta\hat{a}_{out}(\omega) &= A(\omega)\delta\hat{a}_{in}(\omega) + B(\omega)\delta\hat{b}^\dagger_{in}(\omega) & (13)\\ \delta\hat{a}^\dagger_{out}(\omega) &= A^*(-\omega)\delta\hat{a}^\dagger_{in}(\omega) + B^*(-\omega)\delta\hat{b}_{in}(\omega) & (14)\\ \delta\hat{b}_{out}(\omega) &= C^*(-\omega)\delta\hat{a}^\dagger_{in}(\omega) + D^*(-\omega)\delta\hat{b}_{in}(\omega) & (15)\\ \delta\hat{b}^\dagger_{out}(\omega) &= C(\omega)\delta\hat{a}_{in}(\omega) + D(\omega)\delta\hat{b}^\dagger_{in}(\omega) & (16) \end{aligned}$$

We are interested in the situation when the input signal field $\hat{a}$ is a squeezed vacuum state, while the input Stokes field $\hat{b}$ is in a vacuum state. In this case their input quadratures are described as:

$$\begin{aligned} \begin{pmatrix} \langle\delta\hat{x}_{a,in}(\omega)\delta\hat{x}^\dagger_{a,in}(\omega')\rangle & \langle\delta\hat{x}_{a,in}(\omega)\delta\hat{p}^\dagger_{a,in}(\omega')\rangle \\ \langle\delta\hat{p}_{a,in}(\omega)\delta\hat{x}^\dagger_{a,in}(\omega')\rangle & \langle\delta\hat{p}_{a,in}(\omega)\delta\hat{p}^\dagger_{a,in}(\omega')\rangle \end{pmatrix} &= 2\pi\delta(\omega+\omega')\begin{pmatrix} e^{-2r_s} & 0 \\ 0 & e^{2r_s} \end{pmatrix}, & (17)\\ \begin{pmatrix} \langle\delta\hat{x}_{b,in}(\omega)\delta\hat{x}^\dagger_{b,in}(\omega')\rangle & \langle\delta\hat{x}_{b,in}(\omega)\delta\hat{p}^\dagger_{b,in}(\omega')\rangle \\ \langle\delta\hat{p}_{b,in}(\omega)\delta\hat{x}^\dagger_{b,in}(\omega')\rangle & \langle\delta\hat{p}_{b,in}(\omega)\delta\hat{p}^\dagger_{b,in}(\omega')\rangle \end{pmatrix} &= 2\pi\delta(\omega+\omega')\begin{pmatrix} 1 & 0 \\ 0 & 1 \end{pmatrix}, & (18) \end{aligned}$$

where r_s is the squeezing parameter.[11] In this case the relevant expectation values for input fields are:

$$\langle\delta\hat{a}_{in}(\omega)\delta\hat{a}^\dagger_{in}(-\omega')\rangle = \langle\delta\hat{a}^\dagger_{in}(\omega)\delta\hat{a}_{in}(-\omega')\rangle = 2\pi\delta(\omega-\omega')(e^{-2r_s} + e^{2r_s}) \quad (19)$$

and

$$\begin{aligned} \langle\delta\hat{a}_{in}(\omega)\delta\hat{a}_{in}(\omega')\rangle &= -\cosh(r_s)\sinh(r_s)e^{2i\theta_s}2\pi\delta(\omega+\omega') & (20)\\ \langle\delta\hat{a}^\dagger_{in}(\omega)\delta\hat{a}^\dagger_{in}(\omega')\rangle &= -\cosh(r_s)\sinh(r_s)e^{-2i\theta_s}2\pi\delta(\omega+\omega') & (21) \end{aligned}$$

Using the above expressions, we can now evaluate the noise quadratures for the output signal and Stokes fields $S_{a,b,\,out}$:

$$\begin{aligned} S_{a,out}(\omega)\delta(\omega-\omega') &= \frac{1}{2}(|B(\omega)|^2 + |B(-\omega)|^2) + \frac{1}{2}\cosh(2r_s)(|A(\omega)|^2 + |A(-\omega)|^2) \\ &- \sinh(2r_s)\cos(2(\theta_s - \phi_{a,out}))Re(A(\omega)A(-\omega)), \quad (22)\\ S_{b,out}(\omega)\delta(\omega-\omega') &= \frac{1}{2}(|D(\omega)|^2 + |D(-\omega)|^2) + \frac{1}{2}\cosh(2r_s)(|C(\omega)|^2 + |C(-\omega)|^2) \\ &- \sinh(2r_s)\cos(2(\theta_s + \phi_{b,out}))Re(C(\omega)C(-\omega)). \quad (23) \end{aligned}$$

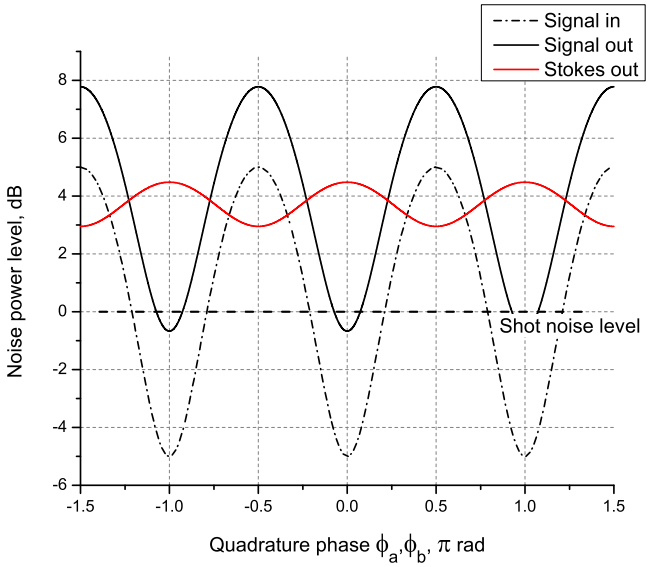

Figure 3. Calculated quadrature noise spectra for input (dashed) and output (solid) signal and Stokes fields at zero sideband frequency as a function of quadrature phases ϕ_a and ϕ_b, correspondingly. The input vacuum Stokes field line is at the shot noise level. Atomic parameters are the same as for Fig. 2.

Fig. 3 illustrates the evolution of quantum noise quadrature noise quadratures after propagation through the atomic medium under EIT-FWM conditions, given by Eqs.(22,23). Input states for the squeezed signal and vacuum Stokes fields are described by Eqs.(17,18) with $r_s = 0.25$. As expected, gain associated with FWM increases overall quantum noise in both quadratures of the signal field. While it is still possible to see some squeezing at the output, it is strongly reduced from $\simeq 5$ dB below the shot noise for the input field to < 1 dB of squeezing at the output. Similar excess noise appears in the Stokes field as well. The quantum noise also becomes phase-dependent, showing that some of the Stokes output originates from the originally squeezed signal field. Nonetheless, the Stokes minimum quadrature does not decrease below the shot noise limit.

To illustrate the increasing influence of the FWM process with atomic density we calculate minimum values of output noise quadratures $S_{a,b}$ for both signal and Stokes fields as functions of optical depth αL, shown in Fig. 4. The extra noise is relatively small for moderate optical depths ($\alpha L \leq 25$). It is interesting to note that in previous experiments with EIT light storage, this is the same range for which the universal optimization procedures[50] were demonstrated to work as predicted for a single Λ system.[42,51,52] As optical depth increases, the quantum noise in both quadratures grows, and after a certain value of the optical depth, both fields exhibit above-shot-noise fluctuations in both noise quadratures.

3. EXPERIMENTAL ARRANGEMENTS

Fig. 5 shows the schematic of the experimental apparatus that has been assembled for the described measurements. It can be roughly separated into three parts: all-atomic squeezed vacuum source, EIT interaction region, and homodyne detection.

3.1 Squeezed vacuum generation

To generate a near-resonant squeezed vacuum signal field for our experiments, we rely on the process of nonlinear polarization self-rotation in Rb vapor.[53–55] This method relies on strong cross-phase modulation between two circularly polarized fields co-propagating in a resonant atomic medium and leads to classical polarization rotation of elliptically polarized light. However, if the incoming field is linearly polarized, the same nonlinear interaction modifies the quantum fluctuations of a vacuum field with orthogonal polarization, which becomes

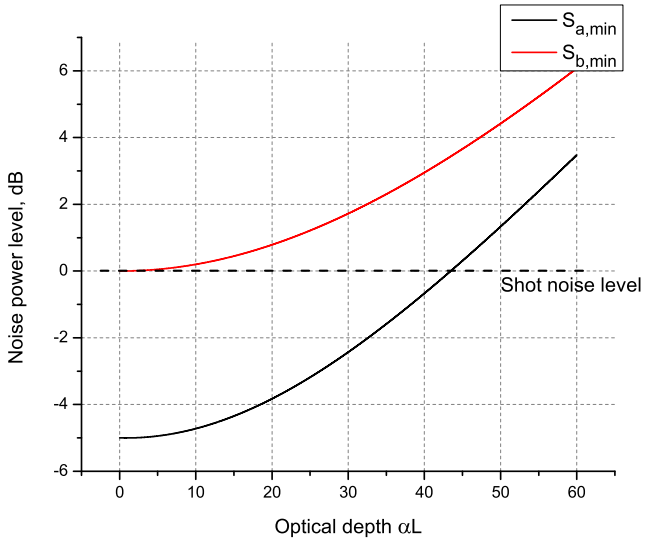

Figure 4. Calculated minimum quadrature noise spectra for output signal and Stokes fields (at zero sideband frequency) as a function of optical depth αL. Atomic parameters are the same as for Fig. 2

squeezed.[53,56–60] In our experiments, we use the output of an external cavity diode laser (ECDL) that is typically tuned to the ^{87}Rb D_1 line $F_g = 2 \rightarrow F_e = 2$ transition and actively locked to this transition using a saturation spectroscopy dither lock. The laser output is then separated: a part of the beam is sent through a polarization-maintaining single mode fiber to achieve a symmetric laser beam with a high-quality Gaussian transverse distribution, and part is used for laser lock and for EIT control optical field generation. After the fiber the laser beam passes through a half-wave plate and a Glan-Laser polarizer (GP), which ensures the purity of its linear polarization and allows for control of the power of the pump laser before entering the squeezing Rb vapor cell. After that, the beam is focused inside the cell with a 40 cm lens (L) to produce a 100μm-wide beam waist in the middle of the *Rb* cell. This configuration, in our experiments, produces the best squeezing (> 2 dB noise suppression below the shot noise limit).

Both squeezing and EIT Rb cells have the same geometry: they are both cylindrical Pirex cells approximately 75 mm long and 22 cm external diameter. The squeezing cell contains only isotopically enriched ^{87}Rb vapor, and the EIT cell also has 2.5 Torr of Ne buffer gas. Each cell is mounted inside a three-layer μ-metal magnetic shield that minimized the influence of stray environmental fields. A solenoid, placed inside the innermost layer of shielding provides precise control over the internal longitudinal magnetic field, that we will use to shape the pulses of squeezed vacuum.[61] After the squeezing cell, the beam is collimated using a second lens with focal length of $f = 300$ mm. The following polarizing beam cube then separates the original laser beam and the squeezed vacuum field (SqV), generated in the orthogonal polarization. The generated squeezed vacuum field is then directed to the EIT cell as a signal field.The pump beam is "recycled" as a local oscillator (LO) for the homodyne detector, since its transverse mode overlaps perfectly with the mode of the squeezed vacuum field.

3.2 EIT interaction

EIT conditions require good phase coherence between the strong control and the squeezed vacuum signal optical fields. To ensure the required relative phase stability, we use the optical fields derived from the same laser whenever possible. To produce the control field for degenerate Zeeman EIT, used for the preliminary measurements, we use two consecutive acousto-optical modulators (AOM). The first one shifts the control field frequency down by -80 MHz, and the second one then shifts it up by $+80 + \delta$MHz, where δ was a controllable small (< 1 MHz) frequency offset, controlled by an external frequency synthesizer. This configuration allows for independent control frequency tuning near the Zeeman resonance. Also, a quater-wave plate is placed immediately before the

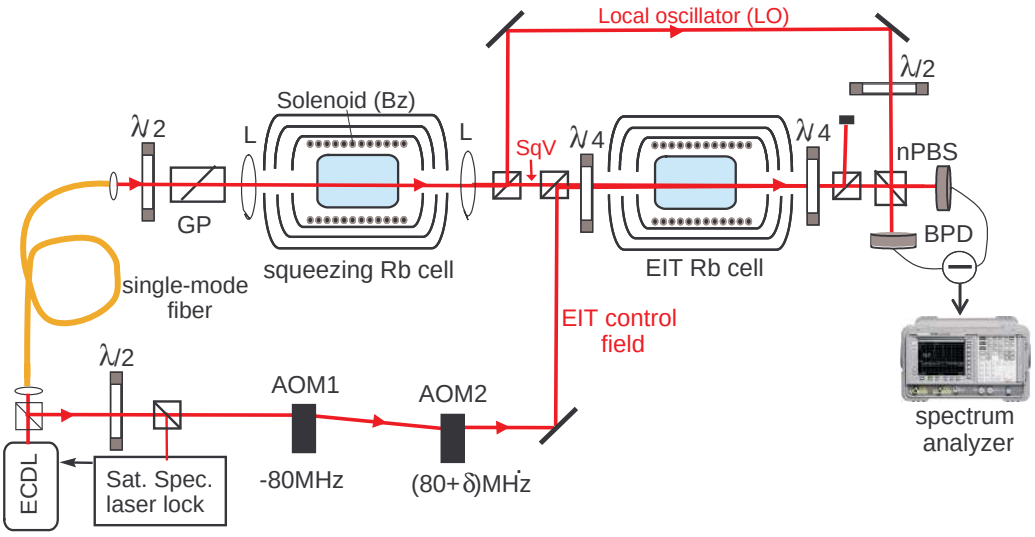

Figure 5. A schematic of the experimental arrangements. See text for abbreviations.

EIT Rb cell, and the degenerate Λ-system is then formed by an orthogonally circular polarized squeezed vacuum signal field and a strong control field.

The linear orthogonally polarized squeezed vacuum signal field and the control field are then overlapped on a polarizing beam splitter before entering the EIT Rb cell, and converted into two orthogonal circular polarizations using a quater wave-plate, placed before the EIT Rb vapor cell. The temperature of the EIT cell, and correspondingly the concentration of Rb in the vapor phase, is controlled using a bifilar resistive heater wound around the inner-most shield layer. For the preliminary experimental data, shown below, the temperature of the cell is maintained at 50°C, which corresponds to a Rb atom number density of 1.1×10^{11} cm^{-3}. After the cell, the signal and control are converted back into orthogonal linear polarizations using a second quater wave-plate.

3.3 Homodyne detection

After the EIT cell, the strong control field is removed using another polarizing beam splitter, and the power spectrum of the signal field quantum noise is recorded using homodyne detection. For that purpose, it is mixed with the local oscillator field that bypasses the EIT Rb cell, at a 50/50 non-polarizing beam splitter(nPBS). The intensities of the resulting two beams are then measured using a home-made balanced photodetector (BPD) with a transimpedance gain of 10^4 V/A, 1 MHz 3 dB bandwidth and electronic noise floor located at 6 dB below shot noise at low frequencies. The BPD incorporates two matched Hamamatsu S3883 photodiodes with quantum efficiency $\eta = 95\%$ and a low noise high bandwidth TI OPA27 operational amplifier. The measured noise spectrum is then detected using a spectrum analyzer.

For measurements of quantum noise of the Stokes field, we will need another local oscillator at the same frequency (shifted by twice the Rb ground-state hyperfine splitting with respect to the original laser frequency). This Stokes LO will be generated in a same or similar vapor cell via the four-wave mixing with non-zero mean input signal field. Measurements of quantum correlations between various quadratures of the signal and Stokes optical fields will be possible by constructing two independent homodyne detectors for each of them, and by simultaneous readings and analysis of intensities for all four photodetectors.

4. PRELIMINARY EXPERIMENTAL DATA

As a preliminary step toward full experimental characterization of quantum noise evolution of the squeezed vacuum signal under EIT-FWM interaction with Rb vapor, we have demonstrated the propagation of a cw squeezed vacuum optical field through the degenerate EIT system, formed via coherence induced between different Zeeman sublevels of the same ground hyperfine state.

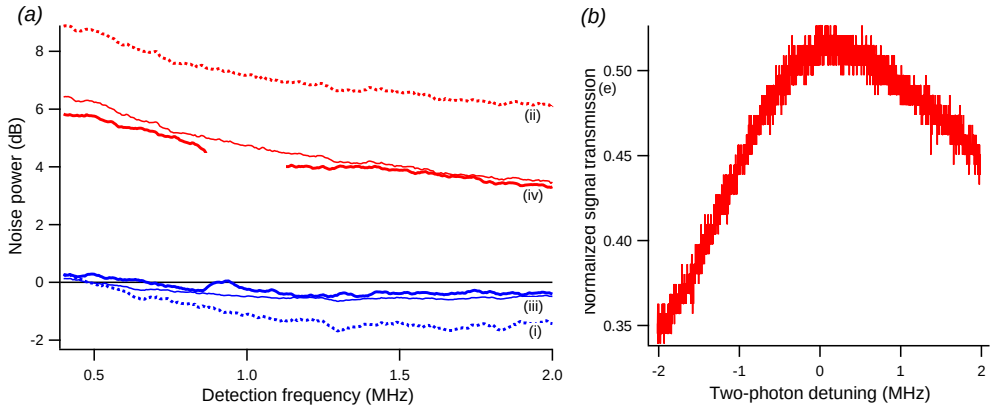

Figure 6. *(a)* Input minimum (i) and maximum (ii), and output minimum (iii) and maximum (iv) signal field quadrature noise power spectra measured before and after the EIT Rb cell, correspondingly. For the output spectra (iii,iv) both experimentally measured (thick lines) and predicted based on input noise and EIT transmission (thin lines) are shown. For these measurements the resolution and video bandwidths were 10 kHz and 30 Hz, correspondingly. Data points around 1 MHz are not shown due to a laser-induced noise peak. *(b)* EIT resonance for a weak coherent signal field.

Fig. 6(a) shows the measured power spectra of two noise quadratures of the squeezed field before and after the EIT Rb cell. For these measurements we adjust the phase of the local oscillator to measure the minimum and maximum of the noise quadratures. We first characterize the input quantum signal field measuring the quadrature noise of the squeezed field after the squeezing Rb cell, maintained at 58.7°C. Using a laser pump power of 21.6 mW, we observed the minimum quadrature noise suppression of approximately 2 dB below the shot noise level. As in previous experiments, we observed large amounts of excess noise.

We have observed squeezing after passing the signal squeezed vacuum field through the EIT Rb cell together with 4.2 mW of control field optical power. The detected squeezing however, was noticeably reduced by the optical losses due to residual EIT absorption. We estimated the expected squeezing spectra using the EIT transmission, measured for a very weak (< 1 μW) classical signal field, shown in Fig. 6(b). The measured maximum transmission is only $\simeq 50$ %, which means that a large fraction of the original squeezed vacuum field has been absorbed and replaced by a coherent vacuum as a result of interaction with Rb atoms. Thin solid lines in Fig. 6(a) show the calculated output spectra based on measured input noise quadratures and the EIT transmission spectrum.[62] We see good agreement between measured and calculated spectra, especially for the anti-squeezed quadrature. The estimated amount of squeezing is slightly below the measured level, indicating that there may be a source of additional noise due to light-atom interaction in the EIT cell, possibly due to the FWM. We will further investigate this in future experiments.

5. CONCLUSION

Here we present theoretical calculations of noise properties of signal and Stokes optical fields propagating through a resonant atomic ensemble in a double-Λ configuration under EIT-FWM conditions. We show that the quantum noise in both fields increases with optical depth, when the FWM process becomes more pronounced. In case of the squeezed vacuum input signal, we see the deterioration of squeezing with the optical depth of the atomic ensemble. The noise quadratures of the generated Stokes field become unbalanced because of the influence of the signal field, but no squeezing is expected for the Stokes field. We also present some preliminary experimental data for propagation of squeezed vacuum field through a Zeeman EIT medium.

ACKNOWLEDGMENTS

The authors thank Nathaniel Phillips and Alexey Gorshkov for useful discussions, and Robinjeet Singh for assistance with the experiment. This research was supported by NSF grant PHY-0758010.

REFERENCES

1. M. Hillery, Phys. Rev. A **61**, 022309 (2000).
2. A. M. Marino, and C. R. Stroud, Phys. Rev. A **74**, 022315 (2006).
3. L. M. Duan, M. D. Lukin, J. I. Cirac, and P. Zoller, Nature **414**, 413 (2001).
4. H. J. Kimble, Nature **453**, 1023-1030 (2008).
5. A. I. Lvovsky, B. C. Sanders and W. Tittel, Nature Photonics **3**, 706 - 714 (2009).
6. K. Hammerer, A. S. Sorensen, E. S. Polzik, Rev. Mod. Phys. **82**, 10411093 (2010).
7. C. Simon, M. Afzelius, J. Appel, A. Boyer de la Giroday, S. J. Dewhurst, N. Gisin, C. Y. Hu, F. Jelezko, S. Kröll, J. H. Müller, J. Nunn, E. S. Polzik, J. G. Rarity, H. De Riedmatten, W. Rosenfeld, A. J. Shields, N. Sköld, R. M. Stevenson, R. Thew, I. A. Walmsley, M. C. Weber, H. Weinfurter, J. Wrachtrup, and R. J. Young, Eur. Phys. J. D **58**, 1-22 (2010).
8. N. J. Cerf, G. Leuchs, and E. S. Polzik, editors. *Quantum Information with Continuous Variables of Atoms and Light*. Imperial College Press, London, 2007.
9. K. Goda, O. Miyakawa, E. E. Mikhailov, S. Saraf, R. Adhikari, K. McKenzie, R. Ward, S. Vass, A. J. Weinstein, and N. Mavalvala, Nature Phys. **4**, 472-476 (2008).
10. F. Wolfgramm, A. Cere, F. A. Beduini, A. Predojevi, M. Koschorreck, and M. W. Mitchell, Phys. Rev. Lett. **105**, 053601 (2010).
11. Hans-A. Bachor and Timothy C. Ralph. *A Guide to Experiments in Quantum Optics*. Wiley-VCH, USA, 2 edition, April 2004.
12. P. M. Anisimov, G. M. Raterman, A. Chiruvelli, W. N. Plick, S. D. Huver, H. Lee, J. P. Dowling, Phys. Rev. Lett. **104**, 103602 (2010).
13. D. F. Phillips, A. Fleischhauer, A. Mair, R. L. Walsworth, and M. D. Lukin, Phys. Rev. Lett. **86**, 783 (2001).
14. B. Julsgaard, J. Sherson, J. Fiurasek, I. Cirac, and E. S. Polzik, Nature **432**, 482 (2004).
15. M. D. Eisaman, A. André, F. Massou, M. Fleischhauer, A. S. Zibrov, and M. D. Lukin, Nature **438**, 837 (2005).
16. M. Hosseini, B. M. Sparkes, P. K. Lam, and B. C. Buchler, Nature Commun. 2:174 doi: 10.1038/ncomms1175 (2011).
17. K. Jensen, W. Wasilewski, H. Krauter, T. Fernholz, B. M. Nielsen, M. Owari, M. B. Plenio, A. Serafini, M. M. Wolf, and E. S. Polzik, Nature Phys. **7**, 13 (2011).
18. K. S. Choi, H. Deng, J. Laurat, and H. J. Kimble, Nature **452**,67-U4 (2008).
19. S. Y. Lan, A. G. Radnaev, O. A. Collins, D. N. Matsukevich, T. A. B. Kennedy, and A. Kuzmich, Opt. Express **17**, 13639-13645 (2009).
20. A. G. Radnaev, Y. O. Dudin, R. Zhao, H. H. Jen, S. D. Jenkins, A. Kuzmich, and T. A. B. Kennedy, Nature Phys. **6**, 894899 (2010).
21. H. Tanji, S. Ghosh, J. Simon, B. Bloom, and V. Vuletic, Phys. Rev. Lett. **103**, 043601 (2009).
22. L.V. Hau, S.E. Harris, Z. Dutton, and C.H. Behroozi, Nature **397**, 594 (1999).
23. R. Zhang, S. R. Garner, and L. V. Hau, Phys. Rev. Lett. **103**, 233602 (2009).
24. J. J. Longdell, E. Fraval, M. J. Sellars, and N. B. Manson, Phys. Rev. Lett. **95**, 063601 (2005).
25. W. Tittel, M. Afzelius, T. Chaneliére, R. L. Cone, S. Kröll, S. Moiseev, and M. Sellars, Laser & Photon. Rev. **4**, 244-267 (2010).
26. M. P. Hedges, J. J. Longdell, Y. Li, and M. J. Sellars, Nature **465**, 1052-1056 (2010).
27. I. Usmani, M. Afzelius, H. de Riedmatten, and N. Gizin, Nature Comm. **1**, 1 (2010).
28. B. Lauritzen, J. Minář, H. de Riedmatten, M. Afzelius, N. Sangouard, C. Simon, and N. Gisin Phys. Rev. Lett. **104**, 080502 (2010).
29. A. A. Abdumalikov, O. Astafiev, A. M. Zagoskin, Y. A. Pashkin, Y. Nakamura, J. S. Tsai, Phys. Rev. Lett. **104**, 193601 (2010).
30. W. R. Kelly, Z. Dutton, J. Schlafer, B. Mookerji, T. A. Ohki, J. S. Kline, and D. P. Pappas, Phys. Rev. Lett **104**, 163601 (2010).
31. M. F. Yanik, W. Suh, Z. Wang, and S. Fan, Phys. Rev. Lett. **93**, 233903 (2004).

32. Q. Xu, P. Dong, and M. Lipson, Nature Phys. **3**, 406-410 (2007).
33. S. Zhang, D. A. Genov, Y. Wang, M. Liu, and X. Zhang,Phys. Rev. Lett. **101**, 047401 (2008).
34. N. Liu, L. Langguth, T. Weiss, J. Kästel, M. Fleischhauer, T. Pfau, and H. Giessen, Nature Materials **8**, 758 - 762 (2009).
35. M. D. Lukin, Rev. Mod. Phys. **75**, 457 (2003).
36. M. Fleischhauer, A. Imamoglu, and J. P. Marangos Rev. Mod. Phys. **77**, 633-673 (2005).
37. I. Novikova, R.L. Walsworth, and Y. Xiao. Laser & Photonics Rev. doi: 10.1002/lpor.201100021 (2011).
38. M. D. Lukin, A. B. Matsko, M. Fleischhauer, and M. O. Scully, Phys. Rev. Lett **82**, 1847-1850 (1999).
39. H. Kang, G. Hernandez, and Y. Zhu, Phys. Rev. A **70**, 061804 (2004).
40. V. Wong, R. S. Bennink, A. M. Marino, R. W. Boyd, C. R. Stroud, and F. A. Narducci, Phys. Rev. A **70**, 053811 (2004).
41. T. Tong, A. V. Gorshkov, D. Patterson, A. S. Zibrov, J. M. Doyle, M. D. Lukin, and M. G. Prentiss, Phys. Rev. A **79**, 013806 (2009).
42. N. B. Phillips, A. V. Gorshkov, and I. Novikova, Phys. Rev. A **78**, 023801 (2008).
43. N. B. Phillips, A. V. Gorshkov, and I. Novikova, J. Mod. Opt. **56**, 1916-1925 (2009).
44. N. B. Phillips, A. V. Gorshkov, and I. Novikova, Phys. Rev. A. **83**, 063823 (2011).
45. R. M. Camacho, P. K. Vudyasetu, and J. C. Howell, Nature Photon. 3, 103-106 (2009).
46. L. Davidovich, Rev. Mod. Phys. **68**, 127 (1996).
47. P. Kolchin, Phys. Rev. A **75**, 033814 (2007).
48. Q. Glorieux, R. Dubessy, S. Guibal, L. Guidoni, J.-P. Likforman, T. Coudreau, and E. Arimondo, Phys. Rev. A **82**, 033819 (2010).
49. K. Drese and M. Holthaus, Eur. Phys. J. D **5** 119134 (1999).
50. A. V. Gorshkov, A. André, M. Fleischhauer, A. S. Sørensen, and M. D. Lukin, Phys. Rev. Lett. **98**, 123601 (2007).
51. I. Novikova, A. V. Gorshkov, D. F. Phillips, A. S. Sørensen, M. D. Lukin, and R. L. Walsworth. Phys. Rev. Lett. **98**, 243602 (2007).
52. Shanchao Zhang, Shuyu Zhou, M. M. T. Loy, G. K. L. Wong, and Shengwang Du. Opt. Lett. **36**, 4530–4532 (2011).
53. A. B. Matsko, I. Novikova, G. R. Welch, D. Budker, D. F. Kimball, and S. M. Rochester. Phys. Rev. A **66**, 043815 (2002).
54. S. M. Rochester, D. S. Hsiung, D. Budker, R. Y. Chiao, D. F. Kimball, and V. V. Yashchuk. Phys. Rev. A **63**, 043814 (2001).
55. I. Novikova, A. B. Matsko, and G. R. Welch. J. Mod. Opt. **49**, 2565–2581 (2002).
56. J. Ries, B. Brezger, and A. I. Lvovsky. Phys. Rev. A **68**, 025801 (2003).
57. Eugeniy E. Mikhailov and Irina Novikova. Opt. Lett. 33,1213–1215 (2008).
58. Eugeniy E. Mikhailov, Arturo Lezama, Thomas W. Noel, and Irina Novikova. J. Mod. Opt. **56**, 1985–1992 (2009).
59. Imad H. Agha, Gaétan Messin, and Philippe Grangier. Opt. Express **18**, 4198–4205(2010).
60. S. Barreiro, P. Valente, H. Failache, and A. Lezama. Phys. Rev. A **84**, 033851 (2011).
61. T. Horrom, I.Novikova and E. E. Mikhailov, submitted to J. Phys. B (2011).
62. E. E. Mikhailov, K. Goda, T. Corbitt, and N. Mavalvala, Phys. Rev. A **73**, 053810, (2006).